

# Topological band theory for non-Hermitian systems from the Dirac equation

Zi-Yong Ge,<sup>1,2</sup> Yu-Ran Zhang,<sup>3,4,\*</sup> Tao Liu,<sup>4,†</sup> Si-Wen Li,<sup>5</sup> Heng Fan,<sup>1,2,6,7,‡</sup> and Franco Nori<sup>4,8</sup>

<sup>1</sup>*Institute of Physics, Chinese Academy of Sciences, Beijing 100190, China*

<sup>2</sup>*School of Physical Sciences, University of Chinese Academy of Sciences, Beijing 100190, China*

<sup>3</sup>*Beijing Computational Science Research Center, Beijing 100193, China*

<sup>4</sup>*Theoretical Quantum Physics Laboratory, RIKEN Cluster for Pioneering Research, Wako-shi, Saitama 351-0198, Japan*

<sup>5</sup>*Department of physics, Dalian Maritime University, Dalian 116026, China*

<sup>6</sup>*CAS Center for Excellence in Topological Quantum Computation, UCAS, Beijing 100190, China*

<sup>7</sup>*Songshan Lake Materials Laboratory, Dongguan 523808, China*

<sup>8</sup>*Department of Physics, University of Michigan, Ann Arbor, Michigan 48109-1040, USA*

We identify and investigate two classes of non-Hermitian systems, i.e., one resulting from Lorentz-symmetry violation (LSV) and the other from a complex mass (CM) with Lorentz invariance. The mechanisms to break, and approaches to restore, the bulk-boundary correspondence in these two types of non-Hermitian systems are clarified. The non-Hermitian system with LSV shows a non-Hermitian skin effect, and its topological phase can be characterized by mapping it to the Hermitian system via a non-compact  $U(1)$  gauge transformation. In contrast, there exists no non-Hermitian skin effect for the non-Hermitian system with CM. Moreover, the conventional bulk-boundary correspondence holds in this (CM) system. We also consider a general non-Hermitian system in the presence of both LSV and CM, and we generalize its bulk-boundary correspondence.

## I. INTRODUCTION

Topological band theory for Hermitian systems, such as topological insulators and topological superconductors [1–14], has made remarkable progress in the past two decades. Recently, topological phases of non-Hermitian systems have been theoretically studied in topological insulators [15–28], topological superconductors [29–33], Weyl semimetals [34–36], etc. [37–54], and have been experimentally observed in Refs. [55–60]. Non-Hermitian Hamiltonians can describe open systems with gain and/or loss [61], interacting and disordered systems with finite lifetimes of quasiparticles [62–65], and have many unique features, e.g., the existence of exceptional points causing eigenstates to coalesce and making Hamiltonians non-diagonalizable [66–71]. Non-Hermitian Hamiltonians have been successfully applied to explain experiments in various platforms including, photonic [72–84] and mechanical systems [85–87]. The introduction of non-Hermiticity into band theory induces many novel topological properties, which are significantly different from their Hermitian counterparts, e.g., Weyl exceptional rings [88], bulk Fermi arcs [89] and breakdown of conventional bulk-boundary correspondence [90–93]. In contrast to the Hermitian case, the bulk spectra of non-Hermitian systems strongly rely on the boundary conditions [91–94]. Therefore, topological invariants, defined by non-Hermitian Bloch

Hamiltonians, usually fail to characterize topological phases in non-Hermitian systems, which leads to the breakdown of the conventional bulk-boundary correspondence. Although many efforts have been made to propose new topological invariants, e.g. non-Bloch winding and Chern numbers [92, 93], to restore the bulk-boundary correspondence of non-Hermitian Hamiltonians [92–96], it remains a challenge to understand and characterize the topological phases of non-Hermitian systems. For example, for a non-Hermitian Hamiltonian, should its topological phase follow the Bloch-wave or non-Bloch-wave behavior? This is not uncovered in Refs. [92, 93].

In this paper, we investigate the topological phases of non-Hermitian systems. According to both Dirac and current-conservation equations, non-Hermitian systems can mainly be classified into two classes: one resulting from Lorentz symmetry violation (LSV), and the other from a complex mass (CM) with Lorentz invariance. We clarify the mechanisms to break the conventional bulk-boundary correspondence in these two types of non-Hermitian systems, and develop approaches to generalize the bulk-boundary correspondence. In particular, the topological phases of non-Hermitian Hamiltonians with LSV can be described by non-Bloch topological invariants, while those with CM follow the Bloch-wave behavior. The non-Hermitian Su-Schrieffer-Heeger (SSH) [97], Qi-Wu-Zhang (QWZ) [98] models and the disordered Kitaev chain [3] exemplify our approaches. Remarkably, our approach can unperturbatively predict the topological phases of 2D non-Hermitian systems. We also discuss a general non-Hermitian system containing *both* LSV and CM non-Hermiticities.

The remaining of this paper is organized as follows. In Sec. II, we give a short review of Hermitian Dirac

---

\* yrzhang@csrc.ac.cn

† tao.liu@riken.jp

‡ hfan@iphy.ac.cn

equation. In Sec. III, the LSV non-Hermitian systems are studied. In Sec. IV, we discuss the non-Hermitian systems with CM. Non-Hermiticity with mixed LSV and CM is discussed in Sec. V. Finally, we summarize the results of this paper in Sec. VI.

## II. HERMITIAN DIRAC EQUATION

Generally, topological band systems can be described by the Dirac equation [12, 99]. The Dirac Hamiltonian reads

$$\mathcal{H} = \bar{\psi}(i\vec{\nabla} \cdot \vec{\gamma} + m)\psi, \quad (1)$$

where  $m$  is the mass of the fermion,  $\psi$  is the field operator of spinors,  $\bar{\psi} = \psi^\dagger \gamma^0$ , and  $\gamma^\mu$ 's satisfy the Clifford algebra  $\{\gamma^\mu, \gamma^\nu\} = 2\eta^{\mu\nu}$ , with  $\eta^{\mu\nu} = \text{diag}\{1, -1, -1, -1\}$  being the Minkowski metric tensor. In addition, we have the conserved current equation

$$\partial_t \rho - \vec{\nabla} \cdot \vec{j} = 0, \quad (2)$$

where  $\rho = \bar{\psi}\gamma^0\psi$  and  $\vec{j} = \bar{\psi}\vec{\gamma}\psi$ . In  $k$  space, the spectrum of Eq. (1) is

$$E_{\pm}^{\text{DE}}(k) = \pm\sqrt{k^2 + m^2}. \quad (3)$$

For  $m = 0$ , there exists zero-energy states, representing the critical points of the topological quantum phase transition. If we consider a domain-wall defect sandwiched by two regions with opposite signs of the mass, there exist gapless boundary modes localized at the interface. In the following sections, we generalize the Hermitian Dirac and current equations to the non-Hermitian cases.

## III. NON-HERMITICITY WITH LSV

In this section, we introduce the first class of non-Hermitian systems, i.e., non-Hermiticity with LSV. We begin with the LSV Dirac equation and then generalize it to the lattice models. We find that the conventional bulk-boundary correspondence of these LSV systems breaks down due to the intrinsic currents, and the non-Hermitian skin effect emerges [92, 93].

### A. Lorentz-symmetry-violation Dirac equation

As  $\mathcal{H}$  is  $U(1)$  gauge invariant, we only need to consider a compact  $U(1)$  gauge group in the Hermitian case. With a specific non-compact  $U(1)$  gauge transformation on  $\mathcal{H}$ , then

$$\mathcal{H}_{\text{LV}} = \bar{\psi}[\vec{\gamma} \cdot (i\vec{\nabla} + \vec{A}) + m]\psi, \quad (4)$$

where  $\vec{A} = \nabla\chi = \vec{A}^r + i\vec{A}^i$  is a complex vector potential, with real vectors  $\vec{A}^r$  and  $\vec{A}^i$ . Here, the non-compact  $U(1)$  gauge transformation  $e^S$  on spinors satisfies

$$\psi \rightarrow e^S \psi, \quad \bar{\psi} \rightarrow \bar{\psi} e^{-S}. \quad (5)$$

In this case,  $\mathcal{H}_{\text{LV}}$  becomes non-Hermitian for  $\vec{A}^i \neq 0$ . Here, the Lorentz symmetry is broken, the compact part of  $U(1)$  gauge symmetry is not broken [100], and we label this type of non-Hermiticity as LSV [101]. The eigenenergies of  $\mathcal{H}_{\text{LV}}$  are real, and have the same values as those of the Hermitian Hamiltonian  $\mathcal{H}$  in spite of the non-Hermitian terms. However, in contrast to the eigenstates of  $\mathcal{H}$ , the real-space right (left) eigenstates of the continuum non-Hermitian Hamiltonian  $\mathcal{H}_{\text{LV}}$  have an extra phase  $e^{-i\chi}$  ( $e^{i\chi}$ ) with complex  $\chi$ . Therefore, the states of  $\mathcal{H}_{\text{LV}}$  become exponentially localized, which is exactly the non-Hermitian skin effect [92, 93]. Furthermore, because  $\mathcal{H}$  and  $\mathcal{H}_{\text{LV}}$  can be transformed to each other by a gauge transformation, they are topologically equivalent.

For non-Hermitian systems, the real-space bands can be considerably different from those in  $k$  space. The eigenenergies of  $\mathcal{H}_{\text{LV}}$  with a constant  $\vec{A}$  in  $k$  space are

$$E_{\pm}^{\text{LSV}}(k) = \pm\sqrt{(\vec{k} + \vec{A}^r + i\vec{A}^i)^2 + m^2}, \quad (6)$$

and can be complex, while they are real in real space. Therefore, the energy spectra of non-Hermitian systems strongly depend on its boundary conditions. Moreover, the bulk-boundary correspondence in this non-Hermitian system with LSV is correspondingly broken.

To uncover the nature of such breakdown, we consider the current equation for  $\mathcal{H}_{\text{LV}}$  [101]:

$$\partial_t \rho - \vec{\nabla} \cdot \vec{j} = -2\vec{A}^i \cdot \vec{j}. \quad (7)$$

The right hand of Eq. (7) is a source term, making the solutions of  $\rho$  and  $\vec{j}$  exponentially localized at the edge with the form  $e^{-i\chi}$  ( $e^{i\chi}$ ). In addition, this source is a classical vector field  $\vec{A}^i$  resulted from non-Hermiticity. To distinguish it with the one in CM case discussed in Sec. IV, we call it an intrinsic current. The intrinsic current suffers from an ambiguity on orientation, when going from open to periodic boundary conditions. This leads to the breakdown of the conventional bulk-boundary correspondence in non-Hermitian system with LSV. To preserve the current conservation and overcome this ambiguity, we replace  $\vec{k}$  with  $(\vec{k} - \vec{A})$  to cancel the effect of the gauge transformation. Then, after applying the Fourier transformation to have a real-space form, the conserved current equation is restored. Moreover, according to topological band theory, the topology relies on the topological properties of the wave function. Thus, the non-compact  $U(1)$  transformation, a local continuous mapping of the wave function, does not change the

topology of the system. Therefore, the topological invariant, defined by the  $k$  space Hamiltonian after replacing  $\vec{k}$  with  $(\vec{k} - \vec{A})$ , reflects the topological phases of  $\mathcal{H}_{LV}$  in real space, which restores the bulk-boundary correspondence.

### B. Lorentz-symmetry-violation lattice models

As in the case for the above continuum model, the topological phases of the lattice model in the presence of the non-Hermiticity with LSV can be also investigated from the perspective of the non-compact  $U(1)$  gauge transformation. To clarify this, we begin with a Hermitian lattice Hamiltonian

$$\mathcal{H}_0 = \sum_{\alpha\beta ij} c_{\alpha,i}^\dagger h_{ij}^{\alpha\beta} c_{\beta,j}, \quad (8)$$

with lattice sites  $i, j$  and band indices  $\alpha, \beta$ . By a non-compact  $U(1)$  gauge transformation [102],  $\mathcal{H}_0$  becomes

$$\tilde{\mathcal{H}} = e^{-S} \mathcal{H}_0 e^S = \sum_{\alpha\beta ij} c_{\alpha,i}^\dagger \tilde{h}_{ij}^{\alpha\beta} \exp(iA_{ij}) c_{\beta,j}, \quad (9)$$

where  $A_{ij}$  is a lattice vector potential. If  $e^S$  is unitary with a real  $A_{ij}$ ,  $\tilde{\mathcal{H}}$  remains Hermitian. However, for the non-unitary transformation  $e^S$  with a complex  $A_{ij}$ ,  $\tilde{\mathcal{H}}$  becomes non-Hermitian with LSV. Moreover, as in the case of the continuum model,  $\tilde{\mathcal{H}}$  exhibits the non-Hermitian skin effect, and breaks the conventional bulk-boundary correspondence. Because  $\tilde{\mathcal{H}}$  and  $\mathcal{H}_0$  are topologically equivalent, the topological phases of the Hamiltonian  $\tilde{\mathcal{H}}$  in the presence of non-Hermiticity with LSV can be characterized by mapping it to the Hermitian form with a non-compact  $U(1)$  gauge transformation.

### C. Two examples

We now consider two concrete 1D and 2D non-Hermitian models with LSV. For the 1D SSH model with an asymmetric intercell hopping:

$$H_1 = \sum_n t_1 c_{A,n}^\dagger c_{B,n} + t_1 c_{B,n}^\dagger c_{A,n} + (t_2 + \Gamma) c_{A,n+1}^\dagger c_{B,n} + (t_2 - \Gamma) c_{B,n}^\dagger c_{A,n+1} \equiv \sum_{\alpha\beta ij} c_{\alpha,i}^\dagger \tilde{h}_{ij}^{\alpha\beta} c_{\beta,j}, \quad (10)$$

where  $\alpha, \beta$  are orbital indices representing the  $A, B$  sublattices, respectively. We rewrite  $H_1$  as

$$H_1 = \sum_{\alpha\beta ij} c_{\alpha,i}^\dagger \tilde{h}_{ij}^{\alpha\beta} \exp(iA_{ij}) c_{\beta,j}, \quad (11)$$

where  $\tilde{h}_{ij}^{\alpha\beta}$  is the standard Hermitian SSH model. Substituting it into Eq. (10), we can obtain

$$A_{ij} = -i \ln \sqrt{(t_2 - \Gamma)/(t_2 + \Gamma)}. \quad (12)$$

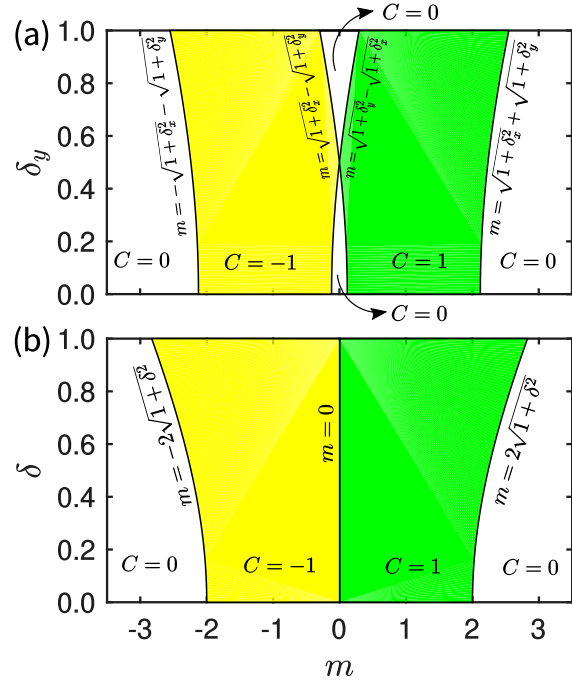


FIG. 1. Phase diagram of the 2D non-Hermitian QWZ model  $H_2$ , with the corresponding Chern numbers  $C_s$ . (a) For the general case, there are four topological phase boundaries with  $m = \pm(\sqrt{1 + \delta_x^2} + \sqrt{1 + \delta_y^2})$ , and  $m = \pm(\sqrt{1 + \delta_x^2} - \sqrt{1 + \delta_y^2})$ . In the vicinity of  $m = 0$ , topologically trivial regions exist. Here,  $\delta_x = 1/2$ . (b) When  $\delta_x = \delta_y = \delta$ , there exist three phase boundaries with  $m = \pm 2\sqrt{1 + \delta^2}$  and  $m = 0$ .

The modified intracell and intercell hopping strengths appearing in  $\tilde{h}_{ij}^{\alpha\beta}$  are

$$\tilde{t}_1 = t_1 \quad \text{and} \quad \tilde{t}_2 = \sqrt{(t_2 - \Gamma)(t_2 + \Gamma)}, \quad (13)$$

respectively. According to the above discussions, the non-Hermitian Hamiltonian  $H_1$  and the transformed Hermitian Hamiltonian

$$\tilde{H}_1 = \sum_{\alpha\beta ij} c_{\alpha,i}^\dagger \tilde{h}_{ij}^{\alpha\beta} c_{\beta,j} \quad (14)$$

are topologically equivalent. Therefore,  $H_1$  is topologically nontrivial for  $-\tilde{t}_2 < t_1 < \tilde{t}_2$ . Note that this generalized bulk-boundary correspondence is the same as the one derived by the non-Bloch-wave method in Ref. [92].

We then consider the 2D non-Hermitian QWZ model [93, 98], which describes a Chern insulator:

$$H_2(\vec{k}) = (\sin k_x + i\delta_x)\sigma_x + (\sin k_y + i\delta_y)\sigma_y + (m - \cos k_x - \cos k_y)\sigma_z. \quad (15)$$

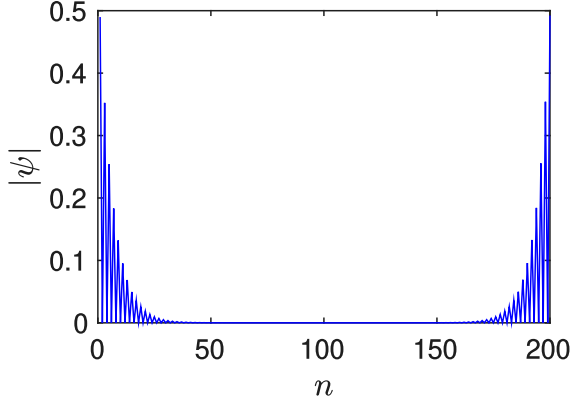


FIG. 2. (Color online). Spatial distribution of the zero-energy modes along the lattice with  $t_1 = 0.4$ . The zero-energy modes are localized at both edges, indicating there is no non-Hermitian effect.

To restore the bulk-boundary correspondence, the non-Bloch-wave method in perturbation theory was used in [93]; while we can solve it exactly. We map  $H_2(\vec{k})$  to the corresponding Hermitian Hamiltonian by a non-compact  $U(1)$  gauge transformation by replacing  $(k_x, k_y)$  with  $(k_x + iA_x, k_y + iA_y)$ . Here, both  $A_x$  and  $A_y$  are real and  $\vec{k}$ -independent, and they can be solved by letting the spectrum of the corresponding Hamiltonian to be real (see Appendix A). Generally, there exist four topological phase boundaries:

$$\begin{aligned} m &= \pm(\sqrt{1 + \delta_x^2} + \sqrt{1 + \delta_y^2}), \\ m &= \pm(\sqrt{1 + \delta_x^2} - \sqrt{1 + \delta_y^2}), \end{aligned} \quad (16)$$

as shown in Fig. 1(a). For the specific case  $\delta_x = \delta_y = \delta$ , three topological phase boundaries can be found as

$$m = 0, \quad \text{and} \quad \pm 2\sqrt{1 + \delta^2},$$

as shown in Fig. 1(b). In particular, for a small  $\delta$ , the topological phase boundaries to first-order approximation are

$$m = \pm(2 + \delta^2), \quad (17)$$

which are consistent with the perturbation results in Ref. [93].

#### IV. NON-HERMITICITY WITH CM

In addition to the non-Hermiticity induced by LSV, the non-Hermiticity can also result from generalizing some parameters from real to complex. One typical example

is the non-Hermitian system whose mass term becomes complex, i.e.,  $m = m^r + im^i$ , with real  $m^r$  and  $m^i$ . In this section, we investigate the topological properties of the non-Hermitian systems with CM. We find that there exists no non-Hermitian skin effect, and the bulk-boundary correspondence holds.

##### A. Complex-mass Dirac equation

The Dirac Hamiltonian of CM system reads

$$\mathcal{H}_{\text{CM}} = \bar{\psi}(i\vec{\nabla} \cdot \vec{\gamma} + m^r + im^i)\psi, \quad (18)$$

which is with Lorentz invariance and compact  $U(1)$  gauge invariance. In contrast to the non-Hermitian Hamiltonian with LSV, it cannot be mapped to the Hermitian form by a non-compact  $U(1)$  gauge transformation. The current equation is calculated as

$$\partial_t \rho - \vec{\nabla} \cdot \vec{j} = 2m^i \gamma^0 \rho. \quad (19)$$

As in the case of LSV, the right hand of Eq. (19) is also a source term resulted from non-Hermiticity, making the solution of  $\rho$  exponentially decay or enhance in the time domain. However, this source term in Eq. (19) is a classical scalar field and not orientable, thus there exists no intrinsic current. Instead, the system decays, and thus behaves like a finite-lifetime particles due to this source. Note that the Hamiltonian Eq. (18) is different from the ones in Refs. [103, 104], where non-Hermitian mass matrices with different symmetries are discussed.

According to the zero-mode domain wall solution of  $\mathcal{H}_{\text{CM}}$ ,  $m^r$  contributes to edge localization, while  $m^i$  leads to oscillations. Therefore,  $m^r = 0$  is the critical point. In  $k$  space, the dispersion relation of  $\mathcal{H}_{\text{CM}}$  is

$$E_{\pm}^{\text{CM}}(k) = \pm\sqrt{k^2 + (m^r + im^i)^2}, \quad (20)$$

where the upper and lower bands coalesce at the exceptional points  $k_{\text{EP}} = \pm|m^i|$  for  $m^r = 0$ , and the topological phase boundaries are determined by  $|E^{\text{CM}}| = 0$ . In contrast to the system with LSV, since the source of non-Hermitian system with CM is not orientable, i.e., there is no intrinsic current, it will not suffer from any ambiguity on orientation, when going from open to periodic boundary conditions. Thus, the energy spectrum is not sensitive to the boundary condition. Therefore, the conventional bulk-boundary correspondence holds for the system in the presence of non-Hermiticity with CM. In Appendix B, we give a detailed geometric description of the topological phase transition for this kind of non-Hermitian system. Note that the above discussion for the non-Hermitian continuum model can be directly generalized to the non-Hermitian lattice model with CM,

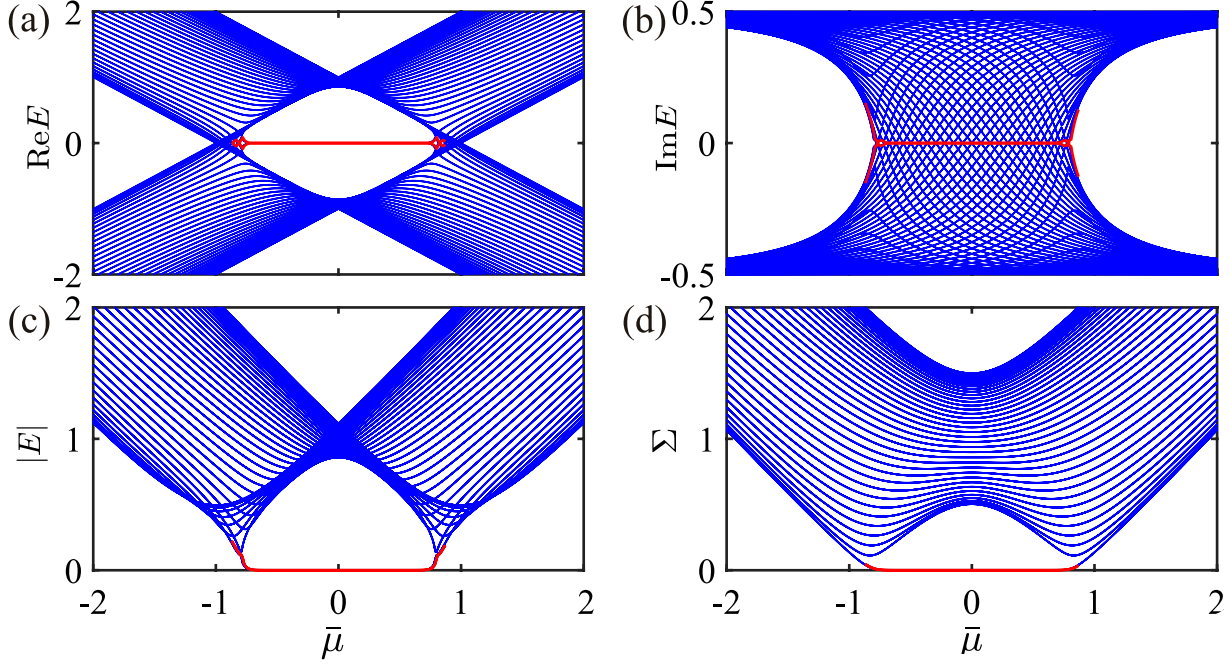


FIG. 3. (a) Real part, (b) imaginary part, (c) absolute values, and (d) singular values of the energy spectra of the effective Hamiltonian  $H_{\text{eff}}(k)$  as a function of  $\bar{\mu}$  with open boundary conditions. For  $|\bar{\mu}| < \sqrt{1 - \Gamma^2} = 0.87$ , the system is topologically nontrivial supporting Majorana zero modes (see red curves). According to the (c,d), the singular values of  $H_{\text{eff}}(k)$  directly reflect the topological phase of the non-Hermitian systems with CM. Here, the number of unit cells is 80, with  $\Gamma = 0.5$ ,  $t = \Delta = 1/2$ , and  $V_0 = 2$ .

where there exists no non-Hermitian skin effect, and the conventional bulk-boundary correspondence holds.

Alternatively, as discussed in Ref. [105], we can consider a minimal coupling to a two-level environment to describe the non-Hermitian systems with CM. The coupled Hamiltonian can be written as

$$H_{cp} = \mathcal{H}_{\text{CM}} \otimes \sigma_+ + \mathcal{H}_{\text{CM}}^\dagger \otimes \sigma_-, \quad (21)$$

where  $\sigma_\pm \equiv (\sigma_x \pm i\sigma_y)/2$ . It is shown that the eigenvalues and eigenvectors of  $H_{cp}$  are the singular values and singular matrices of  $\mathcal{H}_{\text{CM}}$  (see Appendix C). Therefore, the minimal coupling is equivalent to solving the singular value decomposition (SVD) of  $\mathcal{H}_{\text{CM}}$ , where  $|E^{\text{CM}}| = 0$  represents zero-value singular values of  $\mathcal{H}_{\text{CM}}$ . Therefore, we can also use the SVD to explore the topological properties of the non-Hermitian systems with CM, and overcome the precision problem of numerical diagonalization of non-Hermitian Hamiltonians.

### B. Complex-mass SSH model

For a non-Hermitian system with a complex mass, there exists no non-Hermitian skin effect, and the conventional bulk-boundary correspondence holds. To

exemplify this, we consider a non-Hermitian SSH model with complex mass. The real-space Hamiltonian reads

$$H_3 = \sum_n (t_1 + i\kappa) c_{A,n}^\dagger c_{B,n} + (t_1 + i\kappa) c_{B,n}^\dagger c_{A,n} + t_2 c_{A,n+1}^\dagger c_{B,n} + t_2 c_{B,n}^\dagger c_{A,n+1}, \quad (22)$$

whose eigenenergies are complex. It cannot be mapped to a Hermitian model with a non-compact  $U(1)$  gauge transformation. In addition, according to the real-space eigenstates, there exists no non-Hermitian skin effect. Applying the Fourier transformation, we have the  $k$ -space Hamiltonian as

$$\begin{aligned} H_3(k) &= (t_1 + i\kappa + t_2 \cos k) \sigma_x + t_2 \sin k \sigma_y \\ &= \begin{pmatrix} 0 & t_1 + i\kappa + t_2 e^{-ik} \\ t_1 + i\kappa + t_2 e^{ik} & 0 \end{pmatrix} \\ &= \begin{pmatrix} 0 & h_1(k) \\ h_2(k) & 0 \end{pmatrix}. \end{aligned} \quad (23)$$

The dispersion relation is

$$E_\pm(k) = \pm \sqrt{t_1^2 + t_2^2 - \kappa^2 + 2t_1 t_2 \cos k + 2i\kappa(t_1 + t_2 \cos k)}. \quad (24)$$

Letting  $|E_{\pm}(k)| = 0$ , we can obtain the topological phase transition points as  $t_1^2 = t_2^2 - \kappa^2$ . The winding numbers of  $h_1(k)$  and  $h_2(k)$  that have either opposite values or simultaneously zero values. For  $t_1^2 < t_2^2 - \kappa^2$ , the winding numbers are non-zero, indicating that the system is topologically nontrivial. Moreover, the zero-energy boundary modes are localized at both edges (see Fig. 2).

### C. Disordered Kitaev chain

As another concrete non-Hermitian model with CM, we consider a disordered Kitaev chain. The Hamiltonian is  $H_4 = H_0 + H_{\text{dis}}$ , where

$$\begin{aligned} H_0 &= \sum_n [(-tc_{n+1}^\dagger c_n + \Delta c_{n+1}^\dagger c_n^\dagger + h.c.) + \mu c_n^\dagger c_n], \\ H_{\text{dis}} &= \sum_n U_n c_n^\dagger c_n, \end{aligned} \quad (25)$$

where  $H_{\text{dis}}$  denotes diagonal disorder. Here,  $t$  and  $\Delta$  are real numbers representing the hopping strength and the superconducting gap, respectively, and  $U_n \in [-V_0/2, V_0/2]$  is the disorder satisfying a uniform distribution. As shown in Refs. [63–65], we can construct an effective non-Hermitian Hamiltonian by considering the retarded Green's function

$$G_{\text{ret}}(k, \omega) = [\omega - H_{\text{eff}}(k)]^{-1}, \quad (26)$$

where

$$H_{\text{eff}}(k) \equiv H_0(k) + \Sigma_{\text{ret}}(k, \omega), \quad (27)$$

and  $\Sigma_{\text{ret}}(k, \omega)$  is the retarded self-energy of the disorder scattering. The effective Hamiltonian has the form

$$H_{\text{eff}}(k) = -2\Delta \sin k \sigma_y + (\bar{\mu} + i\Gamma - 2t \cos k) \sigma_z, \quad (28)$$

where  $\bar{\mu}$  is a renormalized chemical potential (see Appendix D). This non-Hermitian Hamiltonian effectively describes the disordered Kitaev chain, where the disorder scattering makes the particles possess a finite lifetime, and thus broadens the bands and shrinks the gap [63]. It is thus inferred that the non-Hermiticity in  $H_{\text{eff}}(k)$  is attributed to the CM. The conventional bulk-boundary correspondence holds for  $H_{\text{eff}}(k)$ . The energy spectra of  $H_{\text{eff}}(k)$  is shown in Fig. 3(a-c). When

$$\bar{\mu}^2 < t^2 [4 - (\Gamma/\Delta)^2], \quad (29)$$

the system is topologically nontrivial supporting Majorana zero modes (see red curves). In particular, according to Ref. [106] and Appendix D, for  $\mu = 0$  and  $t = 1$ , the self-energy is  $iV_0^2(\mathbb{1} + \sigma_z)/48$ . The disordered Kitaev chain is topologically nontrivial for

$$|\Delta| > V_0^2/96, \quad (30)$$

which agrees with the results in Refs. [106–108]. In addition, according to Fig. 3(c,d), the singular values of  $H_{\text{eff}}(k)$  directly reflect the topological phase of non-Hermitian systems with CM.

### V. NON-HERMITICITY WITH MIXED LSV AND CM

As discussed above, the non-Hermiticity can mainly result from LSV or CM. However, for a general non-Hermitian system, there exists *both* LSV and CM, dubbed here as mixed non-Hermiticity. In this case, due to LSV, the non-Hermitian system with mixed LSV and CM is sensitive to boundary conditions. Therefore, we need to utilize the non-compact  $U(1)$  gauge transformation to map such mixed non-Hermitian Hamiltonian to the one containing only a CM. Its topological phases are then determined by this transformed Hamiltonian.

We now consider a mixed non-Hermitian SSH model:

$$\begin{aligned} H_5 &= \sum_n [(t_1 + i\kappa + \Gamma)c_{A,n}^\dagger c_{B,n} + (t_1 + i\kappa - \Gamma)c_{B,n}^\dagger c_{A,n} \\ &\quad + t_2 c_{A,n+1}^\dagger c_{B,n} + t_2 c_{B,n}^\dagger c_{A,n+1}]. \end{aligned} \quad (31)$$

By a non-compact  $U(1)$  gauge transformation, we can map it to a non-Hermitian Hamiltonian with the only CM term left as

$$\begin{aligned} \tilde{H}_5 &= e^{-S} H_5 e^S = \sum_n \tilde{t}_1 (c_{A,n}^\dagger c_{B,n} + c_{B,n}^\dagger c_{A,n}) \\ &\quad + \tilde{t}_2 (c_{A,n+1}^\dagger c_{B,n} + c_{B,n}^\dagger c_{A,n+1}), \end{aligned} \quad (32)$$

where [92]

$$e^S = \text{diag}(1, r, r, r^2, r^2, \dots, r^{L-1}, r^{L-1}, r^L), \quad (33)$$

and

$$r = \sqrt{(t_1 + i\kappa - \Gamma)/(t_1 + i\kappa + \Gamma)}, \quad (34)$$

Note that the Hamiltonians  $\tilde{H}_5$  and  $H_5$  are topologically equivalent. The effective intracell and intercell hopping strengths for the transformed Hamiltonian  $\tilde{H}_5$  is obtained as

$$\tilde{t}_1 = \sqrt{(t_1 + i\kappa - \Gamma)(t_1 + i\kappa + \Gamma)} \quad \text{and} \quad \tilde{t}_2 = t_2, \quad (35)$$

respectively. Therefore, for

$$t_1^2 \leq \Gamma^2 - \kappa^2 + \sqrt{t_2^4 - 4\Gamma^2 \kappa^2}, \quad (36)$$

$H_5$  is topologically nontrivial supporting zero-energy boundary modes, as shown in Fig. 4(a,b). The energy spectrum of the mixed non-Hermitian SSH model is sensitive to its boundary conditions [see Fig. 4(b,c)]. In addition, by comparing Fig. 4(c) with 4(d), the singular values of the SVD cannot directly reflect the topological phase of the mixed non-Hermitian systems.

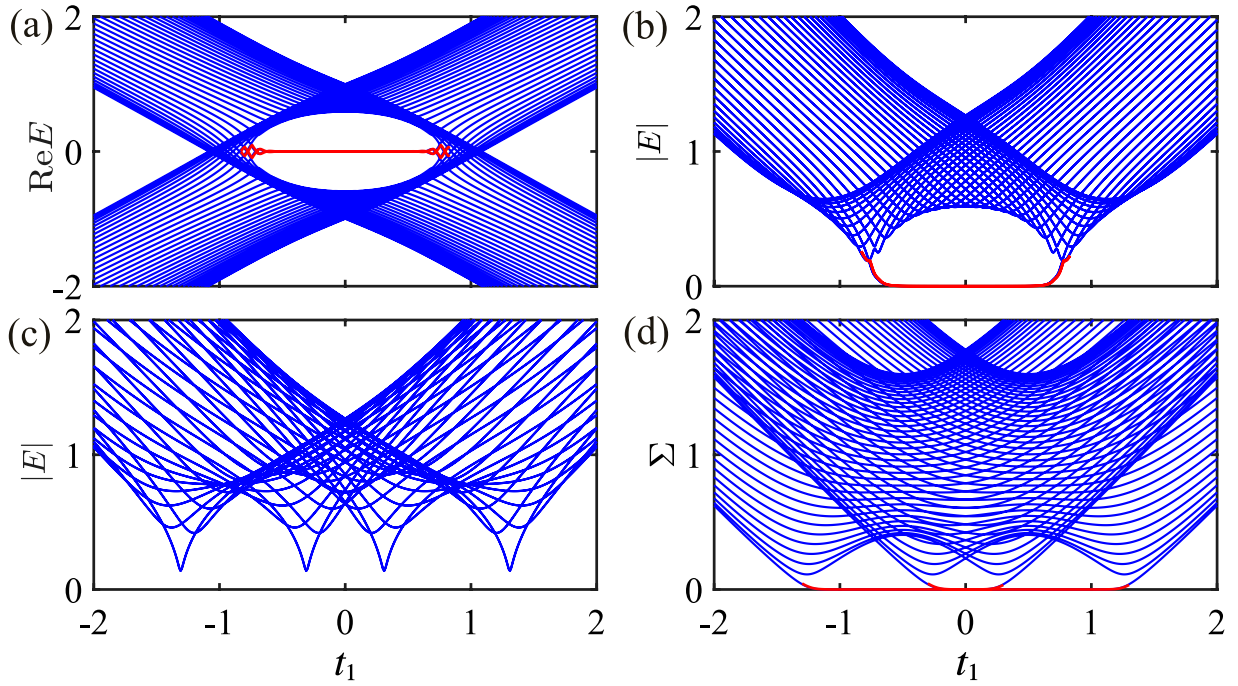


FIG. 4. (a) Real part and (b) absolute value of the energy spectra of  $H_5$  with open boundary conditions. For  $|t_1| < \sqrt{\Gamma^2 - \kappa^2 + (t_2^4 - 4\Gamma^2\kappa^2)^{1/2}} = 0.83$ , the system is topologically nontrivial, supporting zero-energy boundary modes (red curves). The number of unit cells is 80 with  $t_2 = 1$ ,  $\kappa = 0.6$ , and  $\Gamma = 0.5$ . (c) Absolute value of the energy spectrum of  $H_5$  with periodic boundary conditions, where there exists four topological phase transitions. The energy spectrum is distinct from that with open boundary conditions, indicating that the mixed non-Hermitian Hamiltonian is sensitive to its boundary conditions. (d) The singular values of  $H_5$  with the open boundary conditions. According to (b,d), the singular values cannot directly reflect the topological phases of mixed non-Hermitian systems.

## VI. CONCLUSION

The topological phases of non-Hermitian systems are studied from the Dirac equation. Using both Dirac and current-conservation equations, we identified and investigated two classes of non-Hermiticities due to LSV and CM. We also addressed the mechanisms to break the conventional bulk-boundary correspondence in these two types of non-Hermitian systems. There exists intrinsic current and non-Hermitian skin effects in the non-Hermitian system with LSV. The bulk-boundary correspondence can be restored by mapping it to the Hermitian case via a non-compact  $U(1)$  gauge transformation. In contrast, the non-Hermitian system with CM shows no intrinsic current, while the particles in this system have a finite lifetime. Moreover, there exists no non-Hermitian skin effect, and the conventional bulk-boundary correspondence holds in this system. In addition, the singular values of the SVD can be utilized to directly reflect the topological phase of this system. We also studied a general non-Hermitian system containing both LSV and CM non-Hermiticities, and

suggested the approaches to generalize its bulk-boundary correspondence.

## ACKNOWLEDGMENTS

Y.R.Z. was supported by China Postdoctoral Science Foundation (Grant No. 2018M640055) and NSFC (Grant No. U1530401). T.L. was supported by JSPS Postdoctoral Fellowship (P18023). S.W.L. was supported by the research startup foundation of Dalian Maritime University in 2019 and the Fundamental Research Funds for the Central Universities (Grant No. 017192608). H.F. was supported by NSFC (Grant No. 11774406), National Key R & D Program of China (Grant Nos. 2016YFA0302104, 2016YFA0300600), Strategic Priority Research Program of Chinese Academy of Sciences (Grant No. XDB28000000), and Beijing Science Foundation (Grant No. Y18G07). F.N. is supported in part by the: MURI Center for Dynamic Magneto-Optics via the Air Force Office of Scientific Research (AFOSR) (FA9550-14-1-0040), Army Research Office

(ARO) (Grant No. W911NF-18-1-0358), Asian Office of Aerospace Research and Development (AOARD) (Grant No. FA2386-18-1-4045), Japan Science and Technology Agency (JST) (via the Q-LEAP program, the IMPACT program, and the CREST Grant No. JPMJCR1676), Japan Society for the Promotion of Science (JSPS) (JSPS-RFBR Grant No. 17-52-50023, and JSPS-FWO Grant No. VS.059.18N), the RIKEN-AIST Challenge Research Fund, and the John Templeton Foundation.

### Appendix A: Non-Hermitian Qi-Wu-Zhang model with Lorentz symmetry violation

The Qi-Wu-Zhang (QWZ) model is an example of a 2D model describing a Chern insulator. The topological phases of the non-Hermitian QWZ model have been investigated using the non-Bloch-wave method in the framework of perturbation theory in Ref. [93]. However, we can solve it exactly via a non-compact  $U(1)$  gauge transformation. Here, we present the details to obtain the phase diagram of the non-Hermitian QWZ model with the Hamiltonian shown in Eq.(15). By replacing  $\vec{k}$  with  $(\vec{k} + i\vec{A})$ , we have

$$\begin{aligned} \tilde{H}_2(\vec{k}) = & [\sin(k_x + iA_x) + i\delta_x]\sigma_x + [\sin(k_y + iA_y) + i\delta_y]\sigma_y \\ & + [m - \cos(k_x + iA_x) - \cos(k_y + iA_y)]\sigma_z. \end{aligned} \quad (\text{A1})$$

The spectrum of  $\tilde{H}_2(\vec{k})$  can be written as

$$\begin{aligned} E^2 = & [\sin(k_x + iA_x) + i\delta_x]^2 + [\sin(k_y + iA_y) + i\delta_y]^2 + [m - \cos(k_x + iA_x) - \cos(k_y + iA_y)]^2 \\ = & m^2 + 2 - \delta_x^2 - \delta_y^2 + 2i\delta_x(\cosh A_x \cdot \sin k_x + i \sinh A_x \cdot \cos k_x) + 2i\delta_y(\cosh A_y \cdot \sin k_y + i \sinh A_y \cdot \cos k_y) \\ & - 2m(\cosh A_x \cdot \cos k_x - i \sinh A_x \cdot \sin k_x) - 2m(\cosh A_y \cdot \cos k_y - i \sinh A_y \cdot \sin k_y) \\ & + 2(\cosh A_x \cdot \cos k_x - i \sinh A_x \cdot \sin k_x)(\cosh A_y \cdot \cos k_y - i \sinh A_y \cdot \sin k_y). \end{aligned} \quad (\text{A2})$$

Now we consider the real and imaginary parts of  $E^2$  as

$$\begin{aligned} \text{Re}E^2 = & m^2 + 2 - \delta_x^2 - \delta_y^2 - 2\delta_x \sinh A_x \cdot \cos k_x - 2\delta_y \sinh A_y \cdot \cos k_y - 2m \cosh A_x \cdot \cos k_x - 2m \cosh A_y \cdot \cos k_y \\ & + 2 \cosh A_x \cdot \cosh A_y \cdot \cos k_x \cdot \cos k_y - 2 \sinh A_x \cdot \sinh A_y \cdot \sin k_x \cdot \sin k_y, \end{aligned} \quad (\text{A3})$$

$$\begin{aligned} \text{Im}E^2 = & 2\delta_x \cosh A_x \cdot \sin k_x + 2\delta_y \cosh A_y \cdot \sin k_y + 2m \sinh A_x \cdot \sin k_x + 2m \sinh A_y \cdot \sin k_y \\ & - 2 \cosh A_x \cdot \sinh A_y \cdot \cos k_x \cdot \sin k_y - 2 \sinh A_x \cdot \cosh A_y \cdot \sin k_x \cdot \cos k_y. \end{aligned} \quad (\text{A4})$$

By letting  $\text{Im}E^2 = 0$ , we have

$$\delta_x \cosh A_x + m \sinh A_x - \sinh A_x \cdot \cosh A_y \cdot \cos k_y = 0, \quad (\text{A5})$$

$$\delta_y \cosh A_y + m \sinh A_y - \cosh A_x \cdot \sinh A_y \cdot \cos k_x = 0. \quad (\text{A6})$$

Firstly, we consider the special case, i.e.,  $\delta_x = \delta_y = \delta$ . According to Ref. [93], we know that the gapless bands only appear at high-symmetry points of the Brillouin zone, i.e.,  $(k_x, k_y) = (0, 0), (0, \pi), (\pi, 0)$  and  $(\pi, \pi)$ . For  $(k_x, k_y) = (0, 0)$ , according to the symmetry of Eq. (A5) and (A6), we can obtain  $A_x = A_y = A$ , and  $A$  satisfies

$$\delta \cosh A + m \sinh A = \sinh A \cdot \cosh A. \quad (\text{A7})$$

The real part of  $E^2$  can be simplified as

$$\text{Re}E^2 = m^2 + 2 - 2\delta^2 - 4\delta \sinh A - 4m \cosh A + 2 \cosh^2 A. \quad (\text{A8})$$

Given  $\text{Re}E^2 = 0$ , we can solve the Eqs. (A7) and (A8), and the critical point is obtained as

$$m = 2\sqrt{\delta^2 + 1}. \quad (\text{A9})$$

Similarly, for  $(k_x, k_y) = (0, \pi) = (\pi, 0)$ , the corresponding critical point is  $m = 0$ , while for  $(k_x, k_y) = (\pi, \pi)$ , the critical point is

$$m = -2\sqrt{\delta^2 + 1}. \quad (\text{A10})$$

For the general case  $\delta_x \neq \delta_y$ , we can apply the same procedures at the high-symmetry points  $(k_x, k_y) = (0, 0), (0, \pi), (\pi, 0)$  and  $(\pi, \pi)$ . For  $(k_x, k_y) = (0, 0), (\pi, \pi)$ , the critical points can be solved as

$$m = \pm(\sqrt{1 + \delta_x^2} + \sqrt{1 + \delta_y^2}), \quad (\text{A11})$$

and other two critical points are

$$m = \pm(\sqrt{1 + \delta_x^2} - \sqrt{1 + \delta_y^2}). \quad (\text{A12})$$

### Appendix B: Geometric description of topological phase transitions of non-Hermitian systems with complex mass

Here, based on quantum field theory, we give a geometric description of topological phase transitions in Hermitian systems, and then generalize it to the non-Hermitian case with complex mass. This provides a new viewpoint to understand the topological properties of non-Hermitian systems.

In quantum field theory, the 4D Dirac spinor is a representation of the 4D Clifford algebra. The generators of the algebra are  $\gamma^\mu$  matrices, which satisfy

$$\{\gamma^\mu, \gamma^\nu\} = 2\eta^{\mu\nu}. \quad (\text{B1})$$

It mathematically turns out that the 4D Dirac representation of the Lorentz group is reducible due to  $SO(4) \simeq SU_L(2) \times SU_R(2)$ . Hence we can define the chirality with the operator  $P_{L,R} = (1 \mp \gamma_*)/2$ , and  $\psi_{L,R} = P_{L,R}\psi$ . This forms a 2D representation by writing the Dirac spinor as

$$\psi = \begin{pmatrix} \psi_L \\ \psi_R \end{pmatrix}. \quad (\text{B2})$$

Here,  $\psi_{L,R}$  transform under  $SU_{L,R}(2)$ , respectively, and is named as left- and right-handed Weyl spinor. Note that  $\gamma_*$  is defined as  $\gamma_* = i\gamma^0\gamma^1\gamma^2\gamma^3$ , and  $\psi_{L,R}$  are the eigenstates of  $\gamma_*$ . Then let us accordingly consider a global transformation generated by  $\gamma_*$ , i.e., the chiral transformation  $\psi \rightarrow e^{i\theta\gamma_*}\psi$ . Analyzing its infinitesimal transformation, we can obtain the corresponding Noether current  $j_*^\mu = \bar{\psi}\gamma^\mu\gamma_*\psi$ , which satisfies

$$\partial_\mu j_*^\mu = 2im\bar{\psi}\gamma_*\psi. \quad (\text{B3})$$

Note that  $j_*^\mu$  is conserved only if  $m = 0$ , indicating that a chiral phase transition occurs at  $m = 0$ .

Alternatively, there exists a geometric interpretation of the topological or chiral phase transition in fermionic systems. The phase transition could be identified as a Dirac field defined in a space-time with different topologies. Without loss of generality, let us investigate the dynamics of a massless spinor  $\psi(X)$  in  $D + 1$  dimensional Minkowskian spacetime  $\mathbb{R}^{D+1}$  parameterized by  $X \equiv \{X^M\} = \{x^\mu, x^{D+1} \equiv y\}$ , and the index  $\mu$  runs from  $0, 1, \dots, D - 1$ . The Dirac equation for the spinor is given as

$$\gamma^M \partial_M \psi(X) = 0, \quad (\text{B4})$$

where the matrices  $\gamma^M \equiv \{\gamma^\mu, \Gamma\}$  satisfy the  $(D + 1)$  dimensional Clifford algebra  $\{\gamma^M, \gamma^N\} = 2\eta^{MN}$ . In order to take into account a mass term, we could compactify one spatial direction, denoted by  $y$ , of the space-time on a circle  $S^1$  with radius  $L$  so that  $\tau(y) = \tau(y + 2\pi L)$ . Here  $\tau$  denotes the line element on  $S^1$  and the topology of the spacetime now becomes  $\mathbb{R}^D \times S^1$ . Then, we expand the spinor by its Fourier modes as

$$\psi(X) = \sum_n e^{iky} \Psi_n(x), \quad (\text{B5})$$

where  $k$  is the momentum on the  $y$  direction. Note that the boundary condition could be either periodic or anti-periodic, i.e.,  $\psi(x, \tau) = \pm\psi(x, \tau + 2\pi)$  for a spinor, and we consider the anti-periodic condition here, since a fermionic field is not observable. Therefore,  $k$  has to satisfy the quantization condition

$$k = \frac{l}{2L}, \quad l \in Z. \quad (\text{B6})$$

By plugging (B5) into (B4), we obtain

$$\gamma^M \partial_M \psi(X) = \sum_n (\gamma^\mu \partial_\mu + \Gamma \partial_y) e^{iky} \Psi_n(x) = 0, \quad (\text{B7})$$

which leads to

$$(i\gamma^\mu \partial_\mu - k\Gamma) \Psi_n(x) = 0. \quad (\text{B8})$$

Hence we can define the effective mass

$$m_l^2 \equiv |l\Gamma/(2L)|^2 = l^2/(4L^2) \quad (\text{B9})$$

to obtain the massive Dirac equation in  $D$  dimension. As discussed here, the Dirac equation is chirally symmetric only for the massless spinor, so the chiral transition can be geometrically interpreted as going from  $L \rightarrow \infty$  to a finite  $L$ . The former corresponds to a space-time with topology  $\mathbb{R}^{D+1}$ , and the latter corresponds to its topology  $\mathbb{R}^D \times S^1$ . Thus the chiral transition could be understood as a topological transition of the  $(D + 1)$  dimensional spacetime from  $\mathbb{R}^{D+1}$  to  $\mathbb{R}^D \times S^1$ . Furthermore, the equation (B8) also leads to an effective vertex  $k\bar{\Psi}\Gamma\Psi$

in the associated action. If we accordingly compare Eq. (B8) with the coupling term in the gauge theory involving fermions, i.e.,  $\bar{\Psi}\gamma^\mu A_\mu\Psi$ , the effective vertex  $k\bar{\Psi}\Gamma\Psi$  can be obtained by treating  $A_\mu$  as an external field. In this sense, by taking into account the massive Dirac equation

$$(i\gamma^\mu\partial_\mu - m)\Psi(x) = 0, \quad (\text{B10})$$

we can define an imaginary mass,

$$(m^i)^2 \equiv [I\Gamma/(2L)]^2 = -l^2/(4L^2), \quad (\text{B11})$$

in order to describe such an effective interaction in  $D$ -dimensional space-time.

### Appendix C: Minimal coupling and singular value decomposition

The minimal coupling [105] and the singular value decomposition (SVD) can be used to explore the topological properties of the non-Hermitian systems with complex mass. In addition, the SVD can overcome the precision problem of numerically diagonalizing a non-Hermitian Hamiltonian. In this section, we demonstrate that the minimal coupling is equivalent to calculating the singular value decomposition for the non-Hermitian Hamiltonian with complex mass. We write the minimal coupling Hamiltonian

$$H_{cp} = \mathcal{H}_{\text{CM}} \otimes \sigma_+ + \mathcal{H}_{\text{CM}}^\dagger \otimes \sigma_- \quad (\text{C1})$$

as

$$H_{cp} = \begin{pmatrix} 0 & \mathcal{H}_{\text{CM}} \\ \mathcal{H}_{\text{CM}}^\dagger & 0 \end{pmatrix}. \quad (\text{C2})$$

$\mathcal{H}_{\text{CM}}$  satisfies the singular value decomposition as

$$\begin{aligned} \mathcal{H}_{\text{CM}} &= U\Sigma V^\dagger, \\ \mathcal{H}_{\text{CM}}^\dagger &= V\Sigma U^\dagger, \end{aligned} \quad (\text{C3})$$

where  $\Sigma$  is a positive diagonal matrix. Thus, we have

$$H_{cp} = \begin{pmatrix} 0 & U \\ V & 0 \end{pmatrix} \begin{pmatrix} 0 & \Sigma \\ \Sigma & 0 \end{pmatrix} \begin{pmatrix} 0 & V^\dagger \\ U^\dagger & 0 \end{pmatrix}, \quad (\text{C4})$$

with

$$\begin{pmatrix} 0 & \Sigma \\ \Sigma & 0 \end{pmatrix} = \frac{1}{\sqrt{2}} \begin{pmatrix} 1 & 1 \\ -1 & 1 \end{pmatrix} \cdot \begin{pmatrix} -\Sigma & 0 \\ 0 & \Sigma \end{pmatrix} \cdot \frac{1}{\sqrt{2}} \begin{pmatrix} 1 & -1 \\ 1 & 1 \end{pmatrix}. \quad (\text{C5})$$

The Hermitian Hamiltonian  $H_{cp}$  can be diagonalized as

$$H_{cp} = \Lambda \begin{pmatrix} -\Sigma & 0 \\ 0 & \Sigma \end{pmatrix} \Lambda^\dagger, \quad (\text{C6})$$

with

$$\Lambda = \begin{pmatrix} 0 & U \\ V & 0 \end{pmatrix} \cdot \frac{1}{\sqrt{2}} \begin{pmatrix} 1 & 1 \\ -1 & 1 \end{pmatrix}. \quad (\text{C7})$$

It is clear that the eigenvalues and eigenvectors of  $H$  are the singular values and singular matrix of  $\mathcal{H}_{\text{CM}}$ , respectively. Therefore, the minimal coupling is equivalent to solving the singular value decomposition of the non-Hermitian system with complex mass.

### Appendix D: Self-energy of disorder Kitaev chain

To obtain the effective Hamiltonian of the disordered Kitaev chain, we need to calculate the self-energy of the disorder scattering. Here, we derive the form of the self-energy using Feynman diagrams. The Hamiltonian of the disordered Kitaev chain has the form

$$\begin{aligned} H_4 &= \sum_k [\psi_k^\dagger [-2\Delta \sin k\sigma_y + (\mu - 2t \cos k)\sigma_z] \psi_k \\ &+ \sum_q V(q) \psi_{k+q}^\dagger \Lambda \psi_k], \end{aligned} \quad (\text{D1})$$

where  $\psi_k = (c_k, c_{-k}^\dagger)^T$ ,  $V(q) = \sum_n U_n e^{-inq}$ , and  $\Lambda = (\mathbb{1} + \sigma_z)/2$ . In addition,  $V(q)$  satisfies

$$\langle V(q) \rangle = 0, \quad \langle V(q_1)V(q_2) \rangle = \frac{V_0^2}{12} \delta(q_1 + q_2), \quad (\text{D2})$$

where  $\langle \dots \rangle$  means the average over disorder, and  $\delta(\cdot)$  is the Dirac delta function.

We consider the Matsubara self-energy of non-crossing diagrams, and the  $n$ th-order Matsubara self-energy  $\Sigma_n(k, i\omega)$  has the form

$$\begin{aligned} \Sigma_1(k, i\omega) &= \langle V(0) \rangle = 0, \\ \Sigma_2(k, i\omega) &= \sum_q \langle V(k-q)V(q-k) \rangle \Lambda G_0(q, i\omega) \Lambda \\ &\dots \end{aligned} \quad (\text{D3})$$

with

$$G_0(q, i\omega) = \frac{1}{i\omega - H_0(q)}, \quad (\text{D4})$$

where  $H_0(q)$  is the free part of  $H_4$ . Thus, the total Matsubara self-energy reads

$$\Sigma(k, i\omega) = g(k, i\omega) \cdot \Lambda = g(k, i\omega)/2 + g(k, i\omega)/2 \cdot \sigma_z, \quad (\text{D5})$$

where  $g(k, i\omega)$  is a  $(k, \omega)$ -dependent function. By analytic continuation  $i\omega \rightarrow \omega + i0^+$ , we can obtain the

retarded self-energy

$$\begin{aligned}\Sigma_{\text{ret}}(k, \omega) &= \Sigma(k, \omega + i0^+) \\ &= g(k, \omega + i0^+)/2 + g(k, \omega + i0^+)/2 \cdot \sigma_z.\end{aligned}\quad (\text{D6})$$

The real part of  $g(k, \omega + i0^+)$  renormalizes the chemical potential, while the imaginary part gives the finite lifetimes of the particles. Therefore, the effective Hamiltonian of  $H_4$  reads

$$H_{\text{eff}}(k) = -2\Delta \sin k\sigma_y + (\bar{\mu} + i\Gamma - 2t \cos k)\sigma_z, \quad (\text{D7})$$

where

$$\begin{aligned}\bar{\mu} &= \mu + \frac{1}{2}\text{Re}[g(k, \omega + i0^+)], \\ \Gamma &= \frac{1}{2}\text{Im}[g(k, \omega + i0^+)]/2.\end{aligned}\quad (\text{D8})$$

- 
- [1] D. J. Thouless, M. Kohmoto, M. P. Nightingale, and M. den Nijs, Quantized Hall conductance in a two-dimensional periodic potential, *Phys. Rev. Lett.* **49**, 405 (1982).
- [2] N. Read and D. Green, Paired states of fermions in two dimensions with breaking of parity and time-reversal symmetries and the fractional quantum Hall effect, *Phys. Rev. B* **61**, 10267 (2000).
- [3] A. Y. Kitaev, Unpaired Majorana fermions in quantum wires, *Phys. Usp.* **44**, 131 (2001).
- [4] C. L. Kane and E. J. Mele, Quantum spin Hall effect in Graphene, *Phys. Rev. Lett.* **95**, 226801 (2005).
- [5] C. L. Kane and E. J. Mele,  $\mathbb{Z}_2$  Topological order and the quantum spin Hall effect, *Phys. Rev. Lett.* **95**, 146802 (2005).
- [6] J. E. Moore and L. Balents, Topological invariants of time-reversal-invariant band structures, *Phys. Rev. B* **75**, 121306 (2007).
- [7] L. Fu, C. L. Kane, and E. J. Mele, Topological insulators in three dimensions, *Phys. Rev. Lett.* **98**, 106803 (2007).
- [8] L. Fu and C. L. Kane, Topological insulators with inversion symmetry, *Phys. Rev. B* **76**, 045302 (2007).
- [9] A. P. Schnyder, S. Ryu, A. Furusaki, and A. W. W. Ludwig, Classification of topological insulators and superconductors in three spatial dimensions, *Phys. Rev. B* **78**, 195125 (2008).
- [10] A. Y. Kitaev, Periodic table for topological insulators and superconductors, *AIP Conf. Proc.* **22**, 22 (2009).
- [11] M. Z. Hasan and C. L. Kane, Colloquium: topological insulators, *Rev. Mod. Phys.* **82**, 3045 (2010).
- [12] X. L. Qi and S. C. Zhang, Topological insulators and superconductors, *Rev. Mod. Phys.* **83**, 1057 (2011).
- [13] A. Bansil, H. Lin, and T. Das, Colloquium: topological band theory, *Rev. Mod. Phys.* **88**, 021004 (2016).
- [14] C. K. Chiu, J. C. Y. Teo, A. P. Schnyder, and S. Ryu, Classification of topological quantum matter with symmetries, *Rev. Mod. Phys.* **88**, 035005 (2016).
- [15] K. Esaki, M. Sato, K. Hasebe, and M. Kohmoto, Edge states and topological phases in non-Hermitian systems, *Phys. Rev. B* **84**, 205128 (2011).
- [16] Y. C. Hu and T. L. Hughes, Absence of topological insulator phases in non-Hermitian  $\mathcal{PT}$ -symmetric Hamiltonians, *Phys. Rev. B* **84**, 153101 (2011).
- [17] C. Yuce, Topological phase in a non-Hermitian  $\mathcal{PT}$  symmetric system, *Phys. Lett. A* **379**, 1213 (2015).
- [18] M. Klett, H. Cartarius, D. Dast, J. Main, and G. Wunner, Relation between  $\mathcal{PT}$ -symmetry breaking and topologically nontrivial phases in the Su-Schrieffer-Heeger and Kitaev models, *Phys. Rev. A* **95**, 053626 (2017).
- [19] S. Lieu, Topological phases in the non-Hermitian Su-Schrieffer-Heeger model, *Phys. Rev. B* **97**, 045106 (2018).
- [20] C. Yin, H. Jiang, L. Li, R. Lü, and S. Chen, Geometrical meaning of winding number and its characterization of topological phases in one-dimensional chiral non-Hermitian systems, *Phys. Rev. A* **97**, 052115 (2018).
- [21] K. Takata and M. Notomi, Photonic topological insulating phase induced solely by gain and loss, *Phys. Rev. Lett.* **121**, 213902 (2018).
- [22] K. Kawabata, K. Shiozaki, and M. Ueda, Anomalous helical edge states in a non-Hermitian Chern insulator, *Phys. Rev. B* **98**, 165148 (2018).
- [23] T. Liu, Y. R. Zhang, Q. Ai, Z. Gong, K. Kawabata, M. Ueda, and F. Nori, Second-order topological phases in non-Hermitian systems, *Phys. Rev. Lett.* **122**, 076801 (2019).
- [24] L. Jin and Z. Song, Bulk-boundary correspondence in a non-Hermitian system in one dimension with chiral inversion symmetry, *Phys. Rev. B* **99**, 081103 (2019).
- [25] E. Edvardsson, F. K. Kunst, and E. J. Bergholtz, Non-Hermitian extensions of higher-order topological phases and their biorthogonal bulk-boundary correspondence, *Phys. Rev. B* **99**, 081302 (2019).
- [26] C. H. Lee, L. Li, and J. Gong, Hybrid higher-order skin-topological modes in non-reciprocal systems, [arXiv:1810.11824](https://arxiv.org/abs/1810.11824).
- [27] V. M. Martinez Alvarez, J. E. Barrios Vargas, and L. E. F. Foa Torres, Non-Hermitian robust edge states in one-dimension: Anomalous localization and eigenspace condensation at exceptional points, *Phys. Rev. B* **97**, 121401 (2018).
- [28] T. Yoshida, R. Peters, N. Kawakami, and Y. Hatsugai, Symmetry-protected exceptional rings in two-dimensional correlated systems with chiral symmetry, *Phys. Rev. B* **99**, 121101 (2019).

- [29] X. Wang, T. Liu, Y. Xiong, and P. Tong, Spontaneous  $\mathcal{PT}$ -symmetry breaking in non-Hermitian Kitaev and extended Kitaev models, *Phys. Rev. A* **92**, 012116 (2015).
- [30] H. Menke and M. M. Hirschmann, Topological quantum wires with balanced gain and loss, *Phys. Rev. B* **95**, 174506 (2017).
- [31] C. Li, X. Z. Zhang, G. Zhang, and Z. Song, Topological phases in a Kitaev chain with imbalanced pairing, *Phys. Rev. B* **97**, 115436 (2018).
- [32] K. Kawabata, Y. Ashida, H. Katsura, and M. Ueda, Parity-time-symmetric topological superconductor, *Phys. Rev. B* **98**, 085116 (2018).
- [33] K. Kawabata, S. Higashikawa, Z. Gong, Y. Ashida, and M. Ueda, Topological unification of time-reversal and particle-hole symmetries in non-Hermitian physics, *Nat. Commun.* **10**, 297 (2019).
- [34] J. González and R. A. Molina, Topological protection from exceptional points in Weyl and nodal-line semimetals, *Phys. Rev. B* **96**, 045437 (2017).
- [35] A. Cerjan, M. Xiao, L. Yuan, and S. Fan, Effects of non-Hermitian perturbations on Weyl Hamiltonians with arbitrary topological charges, *Phys. Rev. B* **97**, 075128 (2018).
- [36] J. C. Budich, J. Carlström, F. K. Kunst, and E. J. Bergholtz, Symmetry-protected nodal phases in non-Hermitian systems, *Phys. Rev. B* **99**, 041406 (2019).
- [37] M. S. Rudner and L. S. Levitov, Topological transition in a non-Hermitian quantum walk, *Phys. Rev. Lett.* **102**, 065703 (2009).
- [38] J. Gong and Q. H. Wang, Geometric phase in  $\mathcal{PT}$ -symmetric quantum mechanics, *Phys. Rev. A* **82**, 012103 (2010).
- [39] S. D. Liang and G. Y. Huang, Topological invariance and global Berry phase in non-Hermitian systems, *Phys. Rev. A* **87**, 012118 (2013).
- [40] D. Leykam, K. Y. Bliokh, C. Huang, Y. D. Chong, and F. Nori, Edge Modes, degeneracies, and topological numbers in non-Hermitian systems, *Phys. Rev. Lett.* **118**, 040401 (2017).
- [41] Z. Gong, S. Higashikawa, and M. Ueda, Zeno Hall effect, *Phys. Rev. Lett.* **118**, 200401 (2017).
- [42] W. Hu, H. Wang, P. P. Shum, and Y. D. Chong, Exceptional points in a non-Hermitian topological pump, *Phys. Rev. B* **95**, 184306 (2017).
- [43] N. X. A. Rivolta, H. Benisty, and B. Maes, Topological edge modes with  $\mathcal{PT}$  symmetry in a quasiperiodic structure, *Phys. Rev. A* **96**, 023864 (2017).
- [44] H. Shen, B. Zhen, and L. Fu, Topological band theory for non-Hermitian Hamiltonians, *Phys. Rev. Lett.* **120**, 146402 (2018).
- [45] C. H. Lee and R. Thomale, Anatomy of skin modes and topology in non-Hermitian systems, *Phys. Rev. B* **99**, 201103 (2019).
- [46] K. Kawabata, K. Shiozaki, M. Ueda, and M. Sato, Symmetry and topology in Non-Hermitian physics, [arXiv:1812.09133](https://arxiv.org/abs/1812.09133)
- [47] Q. B. Zeng, Y. B. Yang, and Y. Xu, Topological non-Hermitian quasicrystals, [arXiv:1901.08060](https://arxiv.org/abs/1901.08060)
- [48] K. Y. Bliokh, D. Leykam, M. Lein, and F. Nori, Topological non-Hermitian origin of surface Maxwell waves, *Nat. Commun.* **10**, 580 (2019).
- [49] K. Y. Bliokh and F. Nori, Klein-Gordon representation of acoustic waves and topological origin of surface acoustic modes, [arXiv:1902.03614](https://arxiv.org/abs/1902.03614).
- [50] K. Kawabata, T. Bessho, and M. Sato, Non-Hermitian topology of exceptional points, [arXiv:1902.08479](https://arxiv.org/abs/1902.08479).
- [51] H. Zhou and J. Y. Lee, Periodic table for topological bands with non-Hermitian Bernard-LeClair symmetries, [arXiv:1812.10490](https://arxiv.org/abs/1812.10490).
- [52] H. Zhou, J. Y. Lee, S. Liu, and B. Zhen, Exceptional surfaces in  $\mathcal{PT}$ -symmetric non-Hermitian photonic systems, *Optica* **6**, 190 (2019).
- [53] D. S. Borgnia, A. J. Kruchkov, and R.-J. Slager, Non-Hermitian Boundary Modes, [arXiv:1902.07217](https://arxiv.org/abs/1902.07217).
- [54] T. Yoshida, R. Peters, and N. Kawakami, Non-Hermitian perspective of the band structure in heavy-fermion systems, *Phys. Rev. B* **98**, 035141 (2018).
- [55] J. M. Zeuner, M. C. Rechtsman, Y. Plotnik, Y. Lumer, S. Nolte, M. S. Rudner, M. Segev, and A. Szameit, Observation of a topological transition in the bulk of a non-Hermitian system, *Phys. Rev. Lett.* **115**, 040402 (2015).
- [56] X. Zhan, L. Xiao, Z. Bian, K. Wang, X. Qiu, B. C. Sanders, W. Yi, and P. Xue, Detecting topological invariants in nonunitary discrete-time quantum walks, *Phys. Rev. Lett.* **119**, 130501 (2017).
- [57] S. Weimann, M. Kremer, Y. Plotnik, Y. Lumer, S. Nolte, K. G. Makris, M. Segev, M. C. Rechtsman, and A. Szameit, Topologically protected bound states in photonic paritytime-symmetric crystals, *Nat. Mater.* **16**, 433 (2017).
- [58] L. Xiao, X. Zhan, Z. H. Bian, K. K. Wang, X. Zhang, X. P. Wang, J. Li, K. Mochizuki, D. Kim, N. Kawakami, W. Yi, H. Obuse, B. C. Sanders, and P. Xue, Observation of topological edge states in paritytime-symmetric quantum walks, *Nat. Phys.* **13**, 1117 (2017).
- [59] M. Parto, S. Wittek, H. Hodaei, G. Harari, M. A. Bandres, J. Ren, M. C. Rechtsman, M. Segev, D. N. Christodoulides, and M. Khajavikhan, Edge-mode lasing in 1D topological active arrays, *Phys. Rev. Lett.* **120**, 113901 (2018).
- [60] W. Zhu, X. Fang, D. Li, Y. Sun, Y. Li, Y. Jing, and H. Chen, Simultaneous observation of a topological edge state and exceptional point in an open and non-Hermitian acoustic system, *Phys. Rev. Lett.* **121**, 124501 (2018).
- [61] I. Rotter, A non-Hermitian Hamilton operator and the physics of open quantum systems, *J. Phys. Math. Theor.* **42**, 153001 (2009).
- [62] A. A. Zyuzin and A. Y. Zyuzin, Flat band in disorder-driven non-Hermitian Weyl semimetals, *Phys. Rev. B* **97**, 041203 (2018).
- [63] V. Kozii and L. Fu, Non-Hermitian topological theory of finite-lifetime quasiparticles: prediction of bulk Fermi arc due to exceptional point, [arXiv:1708.05841](https://arxiv.org/abs/1708.05841).
- [64] M. Papaj, H. Isobe, and L. Fu, Nodal arc in disordered Dirac Fermions: connection to non-Hermitian band theory, [arXiv:1802.00443](https://arxiv.org/abs/1802.00443).

- [65] H. Shen and L. Fu, Quantum Oscillation from in-gap states and a non-Hermitian Landau level problem, *Phys. Rev. Lett.* **121**, 026403 (2018).
- [66] C. M. Bender and S. Boettcher, Real spectra in non-Hermitian Hamiltonians having  $\mathcal{PT}$  symmetry, *Phys. Rev. Lett.* **80**, 5243 (1998).
- [67] M. V. Berry, Physics of nonhermitian degeneracies, *Czech. J. Phys.* **54**, 1039 (2004).
- [68] W. D. Heiss, The physics of exceptional points, *J. Phys. Math. Theor.* **45**, 444016 (2012).
- [69] R. El-Ganainy, K. G. Makris, M. Khajavikhan, Z. H. Musslimani, S. Rotter, and D. N. Christodoulides, Non-Hermitian physics and  $\mathcal{PT}$  symmetry, *Nat. Phys.* **14**, 11 (2018).
- [70] Ş. K. Özdemir, S. Rotter, F. Nori, and L. Yang, Parity-time symmetry and exceptional points in photonics, *Nat. Mater.*, in press (2019).
- [71] N. Moiseyev, *Non-Hermitian Quantum Mechanics*, (Cambridge University Press, Cambridge, 2011).
- [72] K. G. Makris, R. El-Ganainy, D. N. Christodoulides, and Z. H. Musslimani, Beam dynamics in  $\mathcal{PT}$  symmetric optical lattices, *Phys. Rev. Lett.* **100**, 103904 (2008).
- [73] Y. D. Chong, L. Ge, and A. D. Stone,  $\mathcal{PT}$ -symmetry breaking and laser-absorber modes in optical scattering systems, *Phys. Rev. Lett.* **106**, 093902 (2011).
- [74] A. Regensburger, C. Bersch, M. A. Miri, G. Onishchukov, and D. N. Christodoulides, Parity-time synthetic photonic lattices, *Nature* **488**, 167 (2012).
- [75] H. Jing, Ş. K. Özdemir, X. Y. Lü, J. Zhang, L. Yang, and F. Nori,  $\mathcal{PT}$ -symmetric phonon laser, *Phys. Rev. Lett.* **113**, 053604 (2014).
- [76] H. Hodaie, M. A. Miri, M. Heinrich, D. N. Christodoulides, and M. Khajavikhan, Parity-timesymmetric microring lasers, *Science* **346**, 975 (2014).
- [77] B. Peng, Ş. K. Özdemir, F. Lei, F. Monifi, M. Gianfreda, G. L. Long, S. Fan, F. Nori, C. M. Bender, and L. Yang, Parity-time-symmetric whispering-gallery microcavities, *Nat. Phys.* **10**, 394 (2014).
- [78] L. Feng, Z. J. Wong, R. M. Ma, Y. Wang, and X. Zhang, Single-mode laser by parity-time symmetry breaking, *Science* **346**, 972 (2014).
- [79] B. Peng, Ş. K. Özdemir, S. Rotter, H. Yilmaz, M. Liertzer, F. Monifi, C. M. Bender, F. Nori, and L. Yang, Loss-induced suppression and revival of lasing, *Science* **346**, 328 (2014).
- [80] Z. P. Liu, J. Zhang, Ş. K. Özdemir, B. Peng, H. Jing, X. Y. Lü, C. W. Li, L. Yang, F. Nori, and Y. X. Liu, Metrology with  $\mathcal{PT}$ -symmetric cavities: Enhanced sensitivity near the  $\mathcal{PT}$ -phase transition, *Phys. Rev. Lett.* **117**, 110802 (2016).
- [81] K. Kawabata, Y. Ashida, and M. Ueda, Information retrieval and criticality in parity-time-symmetric systems, *Phys. Rev. Lett.* **119**, 190401 (2017).
- [82] H. Lü, Ş. K. Özdemir, L. M. Kuang, F. Nori, and H. Jing, Exceptional points in random-defect phonon lasers, *Phys. Rev. Applied* **8**, 044020 (2017).
- [83] Y. Ashida, S. Furukawa, and M. Ueda, Parity-time-symmetric quantum critical phenomena, *Nat. Commun.* **8**, 15791 (2017).
- [84] J. Zhang, B. Peng, Ş. K. Özdemir, K. Pichler, D. O. Krimer, G. Zhao, F. Nori, Y. X. Liu, S. Rotter, and L. Yang, A phonon laser operating at an exceptional point, *Nat. Photon.* **12**, 479 (2018).
- [85] H. Jing, Ş. K. Özdemir, Z. Geng, J. Zhang, X. Y. Lü, B. Peng, L. Yang, and F. Nori, Optomechanically-induced transparency in parity-time-symmetric microresonators, *Sci. Rep.* **5**, 9663 (2015).
- [86] H. Jing, Ş. K. Özdemir, H. Lü, and F. Nori, High-order exceptional points in optomechanics, *Sci. Rep.* **7**, 3386 (2017).
- [87] Y. L. Liu, R. Wu, J. Zhang, Ş. K. Özdemir, L. Yang, F. Nori, and Y. X. Liu, Controllable optical response by modifying the gain and loss of a mechanical resonator and cavity mode in an optomechanical system, *Phys. Rev. A* **95**, 013843 (2017).
- [88] Y. Xu, S. T. Wang, and L. M. Duan, Weyl exceptional rings in a three-dimensional dissipative cold atomic gas *Phys. Rev. Lett.* **118**, 045701 (2017).
- [89] H. Zhou, C. Peng, Y. Yoon, Chia W. Hsu, K. A. Nelson, L. Fu, J. D. Joannopoulos, M. Soljačić, and B. Zhen, Observation of bulk Fermi arc and polarization half charge from paired exceptional points, *Science* **359**, 1009 (2018).
- [90] T. E. Lee, Anomalous edge state in a non-Hermitian lattice, *Phys. Rev. Lett.* **116**, 133903 (2016).
- [91] Y. Xiong, Why does bulk boundary correspondence fail in some non-Hermitian topological models, *J. Phys. Commun.* **2**, 035043 (2018).
- [92] S. Yao and Z. Wang, Edge states and topological invariants of non-Hermitian systems, *Phys. Rev. Lett.* **121**, 086803 (2018).
- [93] S. Yao, F. Song, and Z. Wang, Non-Hermitian Chern bands, *Phys. Rev. Lett.* **121**, 136802 (2018).
- [94] F. K. Kunst, E. Edvardsson, J. C. Budich, and E. J. Bergholtz, Biorthogonal bulk-boundary correspondence in non-Hermitian systems, *Phys. Rev. Lett.* **121**, 026808 (2018).
- [95] H. G. Zirnstein, G. Refael, and B. Rosenow, Bulk-boundary correspondence for non-Hermitian Hamiltonians via Green functions, [arXiv:1901.11241](https://arxiv.org/abs/1901.11241).
- [96] L. Herviou, J. H. Bardarson, and N. Regnault, Restoring the bulk-boundary correspondence in non-Hermitian Hamiltonians, [arXiv:1901.00010](https://arxiv.org/abs/1901.00010).
- [97] W. P. Su, J. R. Schrieffer, and A. J. Heeger, Solitons in polyacetylene, *Phys. Rev. Lett.* **42**, 1698 (1979).
- [98] X. L. Qi, Y. S. Wu, and S. C. Zhang, Topological quantization of the spin Hall effect in two-dimensional paramagnetic semiconductors, *Phys. Rev. B* **74**, 085308 (2006).
- [99] S. Q. Shen, *Topological insulators*, (Springer Series in Solid-State Sciences, Springer, New York, 2012).
- [100] X. L. Qi, T. L. Hughes, and S. C. Zhang, Topological field theory of time-reversal invariant insulators, *Phys. Rev. B* **78**, 195424 (2008).
- [101] J. Alexandre and C. M. Bender, Foldy-Wouthuysen transformation for non-Hermitian Hamiltonians, *J. Phys. A: Math. Theor.* **48**, 185403 (2015).

- [102] B. A. Bernevig and T. L. Hughes, *Topological Insulators and topological superconductors*, (Princeton University Press, Princeton, New Jersey, 2013).
- [103] J. Alexandre, C. M. Bender, and P. Millington, Non-Hermitian extension of gauge theories and implications for neutrino physics, *J. High Energy Phys.* **11** (2015) 111.
- [104] K. Jones-Smith and H. Mathur, Relativistic non-Hermitian quantum mechanics, *Phys. Rev. D* **89**, 125014 (2014)
- [105] Z. Gong, Y. Ashida, K. Kawabata, K. Takasan, S. Higashikawa, and M. Ueda, Topological phases of non-Hermitian systems, *Phys. Rev. X* **8**, 031079 (2018).
- [106] P. W. Brouwer, M. Duckheim, A. Romito, and F. von Oppen, Topological superconducting phases in disordered quantum wires with strong spin-orbit coupling, *Phys. Rev. B* **84**, 144526 (2011).
- [107] F. Pientka, G. Kells, A. Romito, P. W. Brouwer, and F. von Oppen, Enhanced zero-bias Majorana peak in the differential tunneling conductance of disordered multisubband quantum-wire/superconductor junctions, *Phys. Rev. Lett.* **109**, 227006 (2012).
- [108] W. DeGottardi, D. Sen, and S. Vishveshwara, Majorana fermions in superconducting 1D systems having periodic, quasiperiodic, and disordered potentials, *Phys. Rev. Lett.* **110**, 146404 (2013).